FATIGUE LIFE PREDICTION IN BENDING

FROM AXIAL FATIGUE INFORMATION

S. S. Manson
Professor, Mechanical and Aerospace Engineering

and

U. Muralidharan
Research Assistant

Case Western Reserve University
Cleveland, Ohio 44106

February 1982

FATIGUE LIFE PREDICTION IN BENDING

FROM AXIAL FATIGUE INFORMATION

S. S. Manson
Professor, Mechanical and Aerospace Engineering

and

U. Muralidharan
Research Assistant

Case Western Reserve University
Cleveland, Ohio 44106

February 1982

INTRODUCTION

It is common to express the bending fatigue life of a material in terms of the nominal elastic stress or strain calculated by assuming stress is proportional to strain. Yet, in the low-cycle fatigue range, and in fact over a wide range of life of engineering interest, plastic flow is involved, and stress is not proportional to strain. Thus considerable discrepancy exists between bending fatigue and axial fatigue when the latter involves expression in terms of true stresses and strains. While several factors contribute to this discrepancy, as discussed in Ref. 1, among them the presence of strain gradient, a volumetric effect, cyclic strain hardening and softening effects, and crack propagation differences after the surface stress has been initiated, the major effect is due to the fact that the nominal stress and strains on a specimen in bending differ considerably from the true values due to plastic deformation.

In Ref. 1, it was demonstrated that flexural fatigue is considerably different from axial fatigue, but that the two could be brought into coincidence when based on true surface stresses. Fig. 1 shows some of the results of the reference. The solid curve and circular data points show the axial fatigue characteristic of 4130 steel. In this case the stresses are true values because in axial loading it is simple to determine the stress from a knowledge of load and cross-sectional area. The dashed curve and square data points refer to the beam bending

characteristics. Here the stress is calculated from the conventional $S = \frac{Mc}{I}$ assumptions, so that the stresses are the fictitious values determined on the basis that no plastic flow occurs. It is seen that for this material the nominal bending stress can be 50% higher at the 100 cycle life level, and that significant difference persists between the two curves until well above 10^5 cycles to failure. Obviously, then, it is important to reconcile the differences over a wide range of life levels of practical engineering interest. It was also demonstrated in Ref. 1, that if the true stress is calculated in the case of the bending specimen the life comparison with the axially loaded comparison is much more favorable. But, because of the difficulty of performing the integrations involved in the bending case no closed-form solution was presented. Each material and geometry had to be treated numerically.

It is the purpose of this report to extend the work of Ref. 1 and to obtain closed-form generalized relationships. The approach is first to study rectangular rather than circular sections. Not only are rectangular sections of great importance in engineering applications, but they result in relations that can be integrated in closed-form. The resulting form of the solutions then provides a model for use in the case of circular sections. By assuming an analogous model, involving several undetermined constants, and then determining the constants so as to fit a range of known solutions obtained by numerical integration, it has been possible to obtain very accurate, though not exact, closed-form solutions for the case of the circular section. The procedure and results will be described in this report.

In addition to the development of plasticity as a reason for
difference between axial and bending fatigue, another factor relating
to volume under stress also introduces differences in the lives of the
two loading modes. In pure axial loading the entire cross section of
the specimen is subjected to the loading stress, whereas in pure bend-
ing only the surface fibers are subjected to the maximum stress, while
other regions of the cross section are subjected to lower stresses.
The effect of this factor is expected to be important in the high cycle
fatigue range, rather than the low cycle fatigue range which is of major
interest in this report. However, this subject is also briefly
discussed.

BASIC EQUATIONS USED FOR LIFE RELATIONSHIPS

The Conventional Life Relationship

The basic model for axial fatigue used in this report is shown in
Fig. 2. Although the model was first proposed by Manson (Ref. 2)
using a different notation, the notation used in Fig. 2 is the one that
has been commonly adopted (Ref. 3). The strain amplitude, $\frac{\Delta t}{2}$ is
plotted on the vertical axis, and the number of reversals $2N_f$ on the
horizontal axis, using logarithmic scales on both axes. If a material
is axially cycled at constant strain range about a zero mean value, or
if the plastic strainrange is maintained constant, it is generally
found that in the early cycles the stress (or, equivalently, the elastic
strain) may change considerably, but eventually a saturation value is

achieved. Usually this saturation value develops early and persists
for the major part of the life of the specimen. Plots such as shown in
Fig. 2, in which both the plastic strain amplitude, and the elastic
strain amplitude, are plotted against reversals to failure result in
straight lines PQ and LM, the equations of which are, respectively,

$$\frac{\Delta\epsilon_p}{2} = \epsilon_f'(2N_f)^c \qquad (1)$$

$$\frac{\Delta\epsilon_e}{2} = \frac{\Delta\sigma}{2E} = \frac{\sigma_f'}{E}(2N_f)^b \qquad (2)$$

where $\Delta\epsilon_p$ is the plastic strainrange, $\Delta\epsilon_e$ is the elastic strainrange,
and $\Delta\sigma$ the saturation stress range, ϵ_f' and $\frac{\sigma_f'}{E}$ are the intercepts
at $2N_f = 1$ of the plastic and elastic lines, E is the elastic modulus, and
c and b are the slopes of the two lines as shown in Fig. 2.

The equation for the total strain amplitude, which is the sum of the
plastic and elastic components, is thus

$$\frac{\Delta\epsilon}{2} = \epsilon_f'(2N_f)^c + \frac{\sigma_f'}{E}(2N_f)^b \qquad (3)$$

In Ref. 4 we introduced the term "transition life" to designate the
life at the intersection point T of the elastic and plastic lines. In
Fig. 2 this life is denoted N_T and the number of reversals is $2N_T$.
Correspondingly, the strainrange at this point is $\Delta\epsilon_T$ and the strain
amplitude is $\Delta\epsilon_{T/2}$. By equating the strains in Eqs. (1) and (2) the
values of N_T and $\Delta\epsilon_T$ can easily be determined.

$$N_T = \frac{1}{2} \left(\frac{E \epsilon_f'}{\sigma_f'} \right)^{\frac{1}{b-c}} \tag{4}$$

$$\Delta \epsilon_T = 2 \left(\epsilon_f' \right)^{\frac{b}{b-c}} \left(\frac{\sigma_f'}{E} \right)^{\frac{c}{c-b}} \tag{5}$$

$$= 2 \left(\epsilon_f' \right)^{\frac{1}{1-n}} \left(\frac{\sigma_f'}{E} \right)^{\frac{n}{n-1}}$$

where $n = \frac{c}{b}$. It may be noted that n is the reciprocal of the strain hardening exponent m' in the relation $\Delta\sigma = $ Constant $(\Delta\epsilon_p)^{m'}$. From Eqs. (4) and (5) it can readily be shown that the basic life model Eq. (3) can be rewritten [5]

$$\frac{\Delta\epsilon}{\Delta\epsilon_T} = \left(\frac{N_f}{N_T} \right)^c + \left(\frac{N_f}{N_T} \right)^b \tag{6}$$

The Inverted Life Relation

For convenience in some of the numerical integration analyses we have also used an alternative form of the life relation discussed in Ref. 6. Basically, life is expressed directly in terms of strain, instead of using Eq. (6) which expresses strain in terms of life

$$\frac{N_f}{N_T} = \left[R_\epsilon^{\frac{z}{c}} + R_\epsilon^{\frac{z}{b}} \right]^{\frac{1}{z}} \tag{7}$$

where

$$z = \exp\left[P \ln^2 R_\varepsilon + Q \ln R_\varepsilon + \ln\left(-.889c \left(\tfrac{c}{b}\right)^{-.36}\right)\right] \tag{8}$$

$$P = -.001277 \left(\tfrac{c}{b}\right)^2 + .03893 \left(\tfrac{c}{b}\right) - .0927 \tag{9}$$

$$Q = +.004176 \left(\tfrac{c}{b}\right)^2 - .135 \left(\tfrac{c}{b}\right) + .2309 \tag{10}$$

$$R_\varepsilon = \frac{\Delta\varepsilon}{\Delta\varepsilon_T} = \text{ratio of strain required to produce life } N_f \text{ to}$$
$$\text{the transition strain} \tag{11}$$

For any material of known b, c, N_T and $\Delta\varepsilon_T$, all the constants involved in the equations are readily calculated, the life N_f is expressed directly in terms of those constants and strainrange.

Similarly, stress range $\Delta\sigma$ can be written directly in terms of applied strainrange $\Delta\varepsilon$

$$\Delta\sigma = E\Delta\varepsilon_T \left[R_\varepsilon^{z/b} + R_\varepsilon^{z/c}\right]^{b/z} \tag{12}$$

The Universal Slopes Life Equation: In cases where material constants b, c, ε'_f and σ'_f are not accurately known from experiment, it may be desired to estimate the life relation on the basis of commonly available material properties. In Ref. 1 it was demonstrated that as a first approximation c could be taken as a universal value of -0.6, b as a universal value of -0.12, and that ε'_f could be estimated from the ductility, while σ'_f was best estimated from ultimate tensile strength. The resulting "universal-slopes" equation, as expressed in Ref. (1), is*,

$$\Delta\varepsilon = D^{0.6} N_f^{-0.6} + \frac{3.5\sigma_u}{E} N_f^{-0.12} \tag{13}$$

---

*While this equation is generally credited only to Manson because it first appeared in Ref. 1, the equal contribution of M. H. Hirschberg in its development is acknowledged.

where

D = ductility = -ln (1-RA) wherein RA is reduction of area in tensile test

σ_u = ultimate tensile strength, and E is elastic modulus in consistent units.

Expressed with the SAE notation of Eq. (3), the equation becomes

$$\frac{\Delta\varepsilon}{2} = 0.7578D^{0.6}(2N_f)^{-0.6} + 1.902 \frac{\sigma_u}{E} (2N_f)^{-0.12} \tag{14}$$

That is, $\varepsilon'_f = 0.7578D^{0.6}$ and $\sigma'_f = 1.902\sigma_u$ $\tag{15}$

Also, using Eqs. (4) and (5),

$$\Delta\varepsilon_T = 4.789 \left(\frac{\sigma_u}{E}\right)^{1.25} D^{-.15} \tag{16}$$

$$N_T = .0735 \left(\frac{\sigma_u}{E}\right)^{-2.083} D^{1.25} \tag{17}$$

so that Eq. (6) becomes

$$\frac{\Delta\varepsilon}{\Delta\varepsilon_T} = \left[\frac{N_f}{N_T}\right]^{-0.6} + \left[\frac{N_f}{N_T}\right]^{-0.12} \tag{18}$$

where $\Delta\varepsilon_T$ and N_T are given by Eqs. (16) and (17), respectively.

Similarly, substituting c = -0.6, b = -0.12 into Eqs. (9) and (10), we obtain P = .07, Q = -.3397

$$z = \exp[.07 \ln^2 R_\varepsilon - .3397 \ln R_\varepsilon - 1.208]$$

$$R_\varepsilon = \frac{\Delta\varepsilon}{\Delta\varepsilon_T}$$

$$N_f = N_T [R_\varepsilon^{z/c} + R_\varepsilon^{z/b}]^{1/z} \tag{19}$$

where $\Delta\varepsilon_T$, N_T are given by Eqs. (16) and (17), respectively.

FLFXURAL BENDING OF RECTANGULAR CROSS-SECTIONS

We first treat the bending of rectangular cross-sections because the resulting equations can be integrated in closed form. As discussed in Ref. 1, it is more convenient to solve this type of problem in an inverse fashion compared to conventional treatment. Rather than starting with a known bending moment, and determining the resulting surface strain--which would involve solution of non-linear equations--it has been found better to select a surface strain and calculate the bending moment required to produce this strain. From the selected surface strain we establish the fatigue life, and from the required bending moment the nominal elastic stress. Thus we can establish the relation between nominal elastic stress and fatigue life.

Fig. 3 shows the notation used in the analysis. We assume a surface strain ϵ_s corresponding to a life N_S when the full bending moment M is applied. Since in bending it is common to assume that plane sections remain plane, strain varies linearly across the thickness, so that the strain ϵ_y at a distance y from the neutral axis (center of bar) is

$$\epsilon_y = \frac{y}{h}\,\epsilon_s \tag{20}$$

Substituting for ϵ_s in terms of life N_S associated with the surface strain, from Eq. (6)[*]

$$\epsilon_y = \frac{y\epsilon_T}{h}\left[\left(\frac{N_S}{N_T}\right)^b + \left(\frac{N_S}{N_T}\right)^c\right] \tag{21}$$

---

[*]Because of the symmetry of loading for this case of completely reversed bending, we omit the Δ's, and consider only surface strains at the maximum loading condition.

Now if N_y is the life associated with the strain at y, then by Eq. (6)

$$\frac{\epsilon_y}{\epsilon_T} = \left(\frac{N_y}{N_T}\right)^b + \left(\frac{N_y}{N_T}\right)^c \tag{22}$$

and the stress associated with the strain ϵ_y is, as derived from Eqs. (2), (4) and (5),

$$\sigma_y = E\ \epsilon_T \left(\frac{N_y}{N_T}\right)^b \tag{23}$$

The increment of bending moment contributed by a strip w dy at the distance y from the neutral axis becomes

$$dM = y \cdot \sigma_y\ w\ dy = E\ \epsilon_T \left(\frac{N_y}{N_T}\right)^b \cdot wy\ dy \tag{24}$$

and the total bending moment, taking into account the symmetrical contribution to bending moment of the section below the neutral axis is

$$M = \int dM = 2Ew\epsilon_T \int_o^{y=h} \left(\frac{N_y}{N_T}\right)^b\ y\ dy \tag{25}$$

Here N_y is a function of y according to Eqs. (21) and (22). In order to carry out the integration it is best to establish dy in terms of $\frac{N_y}{N_T}$, rather than expressing $\frac{N_y}{N_T}$ in terms of y, which would result in a more difficult integration. Thus from Eq. (21) and (22),

$$y = h\ \frac{\left(\frac{N_y}{N_T}\right)^b + \left(\frac{N_y}{N_T}\right)^c}{\left(\frac{N_S}{N_T}\right)^b + \left(\frac{N_S}{N_T}\right)^c} \tag{26}$$

and

$$dy = \frac{h}{\left(\frac{N_S}{N_T}\right)^b + \left(\frac{N_S}{N_T}\right)^c} \left[b\left(\frac{N_y}{N_T}\right)^{b-1} + c\left(\frac{N_y}{N_T}\right)^{c-1} \right] d\left[\frac{N_y}{N_T}\right] \qquad (27)$$

From Eq. (25), therefore,

$$M = \frac{2Ew\,h^2\,\varepsilon_T}{\left[\left(\frac{N_S}{N_T}\right)^b + \left(\frac{N_S}{N_T}\right)^c\right]^2} \int_\infty^{\frac{N_S}{N_T}} \left[b\left(\frac{N_y}{N_T}\right)^{2b-1} + c\left(\frac{N_y}{N_T}\right)^{b+c-1} \right]\left[\left(\frac{N_y}{N_T}\right)^b + \left(\frac{N_y}{N_1}\right)^c \right] d\left(\frac{N_y}{N_T}\right) \quad (28)$$

$$= \frac{2Ew\,h^2\,\varepsilon_T}{\left[\left(\frac{N_S}{N_T}\right)^b + \left(\frac{N_S}{N_T}\right)^c\right]^2} \int_\infty^{\frac{N_S}{N_T}} \left[b\left(\frac{N_y}{N_T}\right)^{3b-1} + b\left(\frac{N_y}{N_T}\right)^{2b+c-1} + c\left(\frac{N_y}{N_T}\right)^{2b+c-1} + c\left(\frac{N_y}{N_T}\right)^{b+2c-1} \right] d\left(\frac{N_y}{N_T}\right)$$

$$(29)$$

$$= \frac{2Ew\,h^2\,\varepsilon_T}{\left[\left(\frac{N_S}{N_T}\right)^b + \left(\frac{N_S}{N_T}\right)^c\right]^2} \left[\frac{b}{3b}\left(\frac{N_y}{N_T}\right)^{3b} + \frac{b+c}{2b+c}\left(\frac{N_y}{N_T}\right)^{2b+c} + \frac{c}{b+2c}\left(\frac{N_y}{N_T}\right)^{b+2c} \right]_{\infty}^{\frac{N_S}{N_T}} \qquad (30)$$

In Eqs. (28), (29) and (30) the lower limit for $\frac{N_y}{N_T}$ is taken at $h = 0$, where the strain is zero, and therefore the life is infinite.

Since all the exponents of $\frac{N_y}{N_T}$ in the integrated expression are negative, the value of all terms is zero at the lower limit, and M is evaluated as

$$M = 2Ew\,h^2\epsilon_T \frac{\frac{1}{3}\left(\frac{N_S}{N_T}\right)^{3b} + \frac{b+c}{2b+c}\left(\frac{N_S}{N_T}\right)^{2b+c} + \frac{c}{b+2c}\left(\frac{N_S}{N_T}\right)^{b+2c}}{\left(\frac{N_S}{N_T}\right)^{2b} + 2\left(\frac{N_S}{N_T}\right)^{b+c} + \left(\frac{N_S}{N_T}\right)^{2c}} \tag{31}$$

The nominal surface stress $S_{bending}$ is $\frac{Mh}{I} = \frac{12Mh}{w(2h)^3} = \frac{12M}{8wh^2}$ since the total height of the rectangle is 2h and the moment of inertia of a rectangular section is $\frac{1}{12}$ base × (height)^3. Thus, substituting for M from Eq. (31), and dividing both numerator and denominator by $\left(\frac{N_S}{N_T}\right)^{2b}$, the resulting equation for $S_{bending}$ is obtained as follows:

$$S_{bending} = E\epsilon_T\left(\frac{N_S}{N_T}\right)^b \left[\frac{1 + \frac{3(b+c)}{2b+c}\left(\frac{N_S}{N_T}\right)^{c-b} + \frac{3c}{b+2c}\left(\frac{N_S}{N_T}\right)^{2(c-b)}}{1 + 2\left(\frac{N_S}{N_T}\right)^{(c-b)} + \left(\frac{N_S}{N_T}\right)^{2(c-b)}} \right] \tag{32}$$

$$S_{axial} = E\epsilon_T\left(\frac{N_S}{N_T}\right)^b \tag{33}$$

$$\frac{S_{bending}}{S_{axial}} = \text{correction factor} = \delta \tag{34}$$

$$\delta = \frac{1 + f_1\left(\frac{N_S}{N_T}\right)^{(c-b)} + f_2\left(\frac{N_S}{N_T}\right)^{2(c-b)}}{1 + 2\left(\frac{N_S}{N_T}\right)^{(c-b)} + \left(\frac{N_S}{N_T}\right)^{2(c-b)}} \tag{35}$$

where

$$f_1 = \frac{3(b+c)}{2b+c} = \frac{1+n}{(2/3)+(1/3)n} \text{ where } n = c/b \qquad (36)$$

$$f_2 = \frac{3c}{b+2c} = \frac{3n}{1+2n} \qquad (37)$$

FLEXURAL BENDING OF CIRCULAR CROSS-SECTIONS

We calculate the bending moment required to produce a selected surface strain. From the selected surface strain fatigue life can be established and similarly nominal stresses from the required bending moment. Thus we establish the relation between nominal elastic stresses and fatigue life.

Figure 4 shows the notation used in the analysis. We assume a surface strain ε_s corresponding to a life N_S when the full bending moment M is applied. Strain varies linearly across the section, so that the strain ε_y at a distance y from the neutral axis is

$$\varepsilon_y = \frac{y}{R} \varepsilon_s$$

$$y = R \sin\theta , \ dy = R \cos\theta d\theta \qquad (38)$$

$$\varepsilon_y = \varepsilon_s \sin\theta \qquad (39)$$

and the stress associated with the strain ε_y can be found using Eq. (12),

$$\sigma_y = E\varepsilon_T \left[\left(\frac{\varepsilon_s \sin\theta}{\varepsilon_T} \right)^{z/b} + \left(\frac{\varepsilon_s \sin\theta}{\varepsilon_T} \right)^{z/c} \right]^{b/z} \qquad (40)$$

where z is given by Eqs. (8) to (11).

The increment of bending moment contributed by a strip at the distance y from the neutral axis becomes

$$dM = y \cdot \sigma_y \cdot (\text{width of the strip}) \cdot dy$$

Substituting for y and dy from Eq. (38) and σ_y from Eq. (40),

$$dM = R \sin\theta \cdot E\varepsilon_T \left[\left(\frac{\varepsilon_s \sin\theta}{\varepsilon_T} \right)^{z/b} + \left(\frac{\varepsilon_s \sin\theta}{\varepsilon_T} \right)^{z/c} \right]^{z/b} 2R\cos\theta \ R\cos\theta \, d\theta \quad (41)$$

The total bending moment, taking into account the symmetrical contribution to bending moment of the section below the neutral axis is

$$M = 2 \int_{y=0}^{y=R} dM$$

$$M = 4R^3 E\varepsilon_T \int_{\theta=0}^{\pi/2} \left[\left(\frac{\varepsilon_s \sin\theta}{\varepsilon_T} \right)^{z/b} + \left(\frac{\varepsilon_s \sin\theta}{\varepsilon_T} \right)^{z/c} \right]^{z/b} \sin\theta \, \cos^2\theta \, d\theta \quad (42)$$

From Eq. (6),

$$\varepsilon_s = \left(\frac{N_S}{N_T} \right)^b + \left(\frac{N_S}{N_T} \right)^c \quad (43)$$

where z is a function of (c/b) and $(\varepsilon_s/\varepsilon_T)$ given by Eqs. (8)-(11).

It is clear from Eq. (42) that the integral does not lend itself to simple closed form solution. However, for any given material and a given surface strain, the integral can be computed numerically and the moment can be calculated. The nominal surface stress $S_{bending}$ is expressed as:

$$S_{bending} = \frac{M\,R}{I} = \frac{M\,R\,64}{\pi R^4} = \frac{64\,M}{\pi R^3} \quad .$$

The ratio of nominal surface stress S to the stress that would be required to produce a life N_S in axial fatigue, can be written analogous to Eq. (35) by assuming the denominator and the exponent (c-b) remain the same for both rectangular and circular cross-sections.

$$\delta = \frac{1 + f_1\left(\dfrac{N_S}{N_T}\right)^{(c-b)} + f_2\left(\dfrac{N_S}{N_T}\right)^{2(c-b)}}{1 + 2\left(\dfrac{N_S}{N_T}\right)^{(c-b)} + \left(\dfrac{N_S}{N_T}\right)^{2(c-b)}} \tag{44}$$

where f_1 and f_2 are for the circular cross-section. The ratio δ is calculated numerically using Eqs. (43) and (42) for different values and combinations of parameters involved as follows:

$$\frac{N_S}{N_T} = 10^{-3}, \ 10^{-2}, \ldots, 10^2, \ 10^3$$

$$c = -0.3, \ 0.4, \ldots, -0.9, -1.0$$

$$b = -.05, -.06, \ldots, -.19, -.20$$

Equation (44) can be written as

$$\delta\left[1 + 2\left(\frac{N_S}{N_T}\right)^{(c-b)} + \left(\frac{N_S}{N_T}\right)^{2(c-b)}\right] = 1 + f_1\left(\frac{N_S}{N_T}\right)^{(c-b)} + f_2\left(\frac{N_S}{N_T}\right)^{2(c-b)} \tag{45a}$$

$$\left\{\frac{\delta\left[1 + 2\left(\frac{N_S}{N_T}\right)^{(c-b)} + \left(\frac{N_S}{N_T}\right)^{2(c-b)}\right] - 1}{\left(\frac{N_S}{N_T}\right)^{(c-b)}}\right\} = f_1 + f_2\left(\frac{N_S}{N_T}\right)^{(c-b)} \tag{45b}$$

$$G\left(\frac{N_S}{N_T}, c, b, \delta\right) = f_1 + f_2 H\left(\frac{N_S}{N_T}, c, b\right) \tag{45}$$

If the function G is plotted against the function H for a given (c/b), i.e. n, but for all combinations of c, b, and $\frac{N_S}{N_T}$, a straight line results. Thus the slope f_2 and intercept f_1 are functions of only n. The plot of G vs. H for different n values are shown in Fig. 5. For clarity the numerical values of functions G and H for different combinations of c, b and N_S/N_T are shown in Fig. 5 only for the case of $n = 5$. The above procedure is repeated for several materials of various n values and the parameters f_1 and f_2 are calculated for each material with a specific n They are shown in Fig. 6.

Since the parameters f_1 and f_2 are found to be functions of only n, an attempt was made to determine these functions whose form is analogous to ones shown for rectangular cross-section in Eqs. (36) and (37). The functions were determined by least squares analysis to be

$$f_1 = \frac{1 + .8432\ n}{.6849 + .255\ n} \tag{46}$$

$$f_2 = \frac{2.6188\ n}{1 + 1.5411\ n} \tag{47}$$

The curves represented by the above functions are shown by solid lines in Figure 6.

For any given material the functions f_1 and f_2 can be calculated using the reciprocal of the strain hardening exponent, n, and Eqs. (46) and (47). The correction factor δ and axial stress S_{axial} can be calculated for any given life using Eqs. (44) and (33), respectively. Thus we can plot nominal bending stress $S_{bending}$ against life. The plots are shown in Fig. 7

for several materials of engineering interest. The properties of these materials, obtained from Ref. 7, are listed in Table II.

If the fatigue properties of the material are not known or cannot be obtained easily, Universal Slopes solutions can be used with the properties obtained from a tensile test. Universal plastic and elastic exponents of -0.6 and -0.12 are used, respectively. Transition strain ϵ_T and transition life N_T can be determined from Eqs. (16) and (17), respectively.

DISCUSSION

The approach presented in this report takes into account only the effect of plastic flow in explaining the difference between axial and bending fatigue lives; hence, it is valid in the low cyclic life range. According to the analysis, the S_{axial} and $S_{bending}$ curves become coincident for most engineering materials at lives greater than 10^6 cycles since the strains are purely elastic at those life levels and the Mc/I assumption is valid. However, bending fatigue life could still be higher than at axial fatigue for the same nominal stress due to volumetric effect which is not taken into account in the current approach. This is observed by Esin in steels and he has used micro-plastic strain energy criterion to take this factor into account (Ref. 8). This is also discussed in some detail in connection with risk-of-rupture criterion in Ref. 9. Basically, in bending fatigue lower volume of material is under high strain at outer fibers as compared to the whole volume in the axial case. Thus, the smaller the volume under maximum stress,

the lower will be the probability of the presence of a flaw at a point of high stress, hence the higher will be the life.

At high cyclic life range, the rotating bending will give lower life as compared to alternating bending for the same nominal stress which can e explained as follows. In alternating bending the regions A and B in Fig. 4 will be subjected to maximum surface strain, whereas in rotating bending all the material near the surface of the cylinder will be subject to maximum strain at different times; for example, the region C will take the position of A or B while rotating, hence will be subjected to maximum strain. Thus, more volume is subjected to high stress in rotating bending hence greater will be the probability of the presence of a flaw at a point of high stress and lower will be the life.

It should be noted that results obtained in this report are valid for alternating flexural bending. If the material is subjected to rotating bending, the cross-section deflects about a different axis, which makes an angle with the loading axis (Ref. 1). Once the angle between two axes is determined, the complete stress and strain distribution can be computed from which the bending moment for an assumed value of maximum surface strain can be established. In Ref. 1 it was observed that although the analysis for rotating bending is considerably more complicated than static flexural bending, the resulting strain distributions for the two cases differed little when considered in their respective bending planes. It was shown that the experimental results for rotating bending agreed well with the predictions made for static flexural bending. Hence it will be assumed here that the equations for flexural bending, Eq. (44) together with the f_1 and f_2 values given in Eqs. (46) and (47), are also valid for rotating bending in the low cycle fatigue range. Further study may be desirable to verify this assumption.

CONCLUSION

Closed-form expressions were obtained for nominal bending stress in terms of axial fatigue stress based on true surface stresses. They are shown for rectangular and circular cross-sections in Table I. Using only axial fatigue data on a given material and formulas given in Table I, nominal bending stress-life curve can be established. Though the study is limited to only rectangular and circular cross-sections, the approach and the procedure described in this report can be applied to more complicated geometries to obtain the functional forms for parameters f_1 and f_2 which are functions of only strain hardening exponent of the material. The approach takes into account only the effect due to plastic flow which has dominating effect in the low cyclic life range. However, in the high cyclic life range other factors could be more dominating like the volumetric effect which should be taken into account in reconciling the difference between axial and bending fatigue lives. Future study is necessary to incorporate the volumetric effect in the analyses presented in this report.

REFERENCES

1. Manson, S.S., "Fatigue: A Complex Subject - Some Simple Approximations."
   Proceedings Society of Experimental Stress Analysis 12, No. 2 (1965).

2. Manson, S.S., "Thermal Stress in Design, Part 19, Cyclic Life of Ductile
   Materials," Machine Design (July 7, 1960), pp. 139-144.

3. Morrow, J., "Cyclic Plastic Strain Energy and Fatigue of Metals,"
   ASTM STP 378 (1965), pp. 45-87.

4. Smith, R.W., Hirschberg, M.H., and Manson, S.S., "Fatigue Behavior of
   Materials Under Strain Cycling in Low and Intermediate Life Range,"
   NASA-TN-D-1574, April 1963.

5. Manson, S.S., "Predictive Analysis of Metal Fatigue in the High Cycle
   Life Range," Methods for Predicting Material Life in Fatigue, The
   Winter Annual Meeting of the ASME Dec. 2-7, 1979, pp. 145-183.

6. Manson, S.S. and U. Muralidharan, "A Single Expression Formula for
   Inverting Strain-Life and Stress-Strain Relationships," NASA CR-165347.

7. Landgraf, R.N., Mitchell, M.R. and LaPointe, N.R., "Monotonic and Cyclic
   Properties of Engineering Materials," Ford Motor Company (1972).

8. Esin, A., "A method for correlating different types of fatigue curve,"
   International Journal of Fatigue, Vol. 2, No. 4, Oct. 1980, pp. 153-158

9. Manson, S.S., "Thermal Stress and Low-cycle Fatigue," Robert E. Kreiger
   Publishing Company, Malabar, Florida, 198 , sec. 7.1.7 and 7.1.8.

TABLE I

$n = c/b$ ratio of plastic to elastic exponents

ϵ_T = transition strain range = $2\epsilon_f'^{\frac{1}{1-n}}\left(\frac{\sigma_f'}{E}\right)^{\frac{n}{n-1}}$

where ϵ_f' = fatigue ductility coefficient

σ_f' = fatigue strength coefficient

E = modulus of elasticity

N_T = Transition life = $\frac{1}{2}\left(\frac{E\epsilon_f'}{\sigma_f'}\right)^{\frac{1}{b-c}}$

S_{axial} = $E\epsilon_T\left(\frac{N_S}{N_T}\right)^b$

$$S_{bending} = \left[\frac{1 + f_1\left(\frac{N_S}{N_T}\right)^{(c-b)} + f_2\left(\frac{N_S}{N_T}\right)^{2(c-b)}}{1 + 2\left(\frac{N_S}{N_T}\right)^{(c-b)} + \left(\frac{N_S}{N_T}\right)^{2(c-b)}}\right] S_{axial}$$

where f_1 and f_2 are functions of n and depend on the geometry of the cross-section.

For Rectangular Section

$f_1 = \frac{1 + n}{(2/3) + (1/3)n}$

$f_2 = \frac{3n}{1 + 2n}$

For Circular Cross-section

$f_1 = \frac{1 + .8432\ n}{.6849 + .255\ n}$

$f_2 = \frac{2.6188\ n}{1 + 1.5411\ n}$

For any given surface strain ϵ_s, surface life N_s can be found from Fig. 2 and S_{axial} and $S_{bending}$ can be computed using the above formulas.

Table Ii

1 MATERIAL	2 σ'_f ksi	3 ϵ'_f	4 b	5 c	6 E ksi	7 $S\epsilon_T$	8 N_T Cycles
#1 SAE1005-1009 HRLC	78	.11	-.073	-.41	29000	2.41×10^{-4}	30300
#2 GAINEX (HRLC)	117	.86	-.071	-.65	29200	4.15×10^{4}	5322
#3 MAN-TEN-150BHN	141	.85	-.11	-.59	30000	2.86×10^{-x}	2521.9
#4 SAE1045-225 BHN	178	1.0	-.095	-.66	29000	$5.21 \times .?$	4111
#5 SAE1045-390 BHN	230	.45	-.074	-.68	30000	$9.33 \times 1.?$	4.4
#6 SAE1045-410 BHN	270	.60	-.073	-.70	29000	.01146	384
#7 SAE1045-450 BHN	260	.35	-.07	-.69	30000	.01142	195
#8 SAE1045-595 BHN	395	.07	-.081	-.60	30000	.0203	12.5
#9 10B62-430 BHN	258	.32	-.067	-.56	28000	.0114	667
#10 AISI4130-365 BHN	246	.89	-.081	-.69	29000	$9.14 \times 10^{-?}$	1041
#11 SAE4142-475 BHN	315	.09	-.081	-.61	30000	.01511	29
#12 SAE4142-560 BHN	385	.07	-.089	-.76	30000	.0205	6.27
#13 TI-6AL-4V	552.4	1.053	-.1052	-.6903	17000	.0348	191
#14 SAE4142-400 BHN	275	.5	-.09	-.75	29000	.011	201.3
#15 SAE4142-450 BHN	290	.40	-.08	-.73	30000	.0122	154
#16 SAE4142-475 BHN	300	.20	-.082	-.77	29000	.0145	37
#17 AISI4340-243 BHN	174	.45	-.095	-.54	28000	$4.98 \times 10^{-?}$	7557
#18 AISI4340-409 BHN	290	.68	-.091	-.60	29000	.01	1005
#19 SAE5160-430 BHN	280	.40	-.071	-.57	28000	.0118	812
#20 SAE9262-260 BHN	151	.155	-.071	-.47	30000	$5.47 \times 10^{-?}$	2688
#21 SAE9262-410 BHN	269	.38	-.057	-.65	29000	.013	262
#22 AISI304-160 BHN	350	1.02	-.15	-.77	27000	$9.02 \times 10^{-?}$	571.3
#23 AISI310-145 BHN	240	.60	-.15	-.57	28000	$3.76 \times 10^{-?}$	1234?
#24 AM350 Annealed	406	.33	-.14	-.84	28000	.016	43.4
#25 18% Ni-Maraging 440 BHN	310	.80	-.071	-.79	27000	.015	183

Table II (Continued)

1	2	3	4	5	6	7	8
MATERIAL	σ'_f ksi	ε'_f	b	c	E ksi	$\Delta\varepsilon_T$	N_T Cycles
#26 18% Ni-Maraging 480 BHN	325	.60	-.07	-.75	26000	.017	.48
#30 2014-Al-T6	123	.42	-.106	-.65	10000	.0124	329
#31 2014-Al-T4	147	.21	-.11	-.52	10200	.0140	344
#32 5456 Aluminum	105	.46	-.11	-.67	10000	9.99×10	427
#33 SAE1015-80 BHN	120	.95	-.11	-.64	30000	2.57×10	15183
#34 SAE950X-150 BHN	91	.35	-.075	-.54	30000	2.82×10	13604
#35 VAN80-225 BHN	153	.21	-.08	-.53	28200	5.67×10	1688
#36 RQC100-290 BHN	147	.60	-.076	-.47	29400	5.42×10	1502
#37 SAE1045-500 BHN	330	.25	-.08	-.68	30000	.0145	91
#38 AISI4130-258 BHN	185	.92	-.083	-.63	32000	5.36×10	5298
#39 SAE4142-380 BHN	265	.45	-.08	-.75	30000	.0110	177
#40 SAE4142-450 BHN	305	.60	-.09	-.76	29000	.0122	209
#41 SAE4340-350 BHN	240	.73	-.076	-.62	28000	9.21×10	1767
#42 AISI52100-518 BHN	375	.18	-.09	-.56	30000	.015	146
#43 SAE9262-280 BHN	177	.41	-.073	-.60	28000	7.09×10	1372
#44 H-11 660 BHN	460	.08	-.077	-.74	30000	.0253	6
#45 AISI304-327 BHN	330	89	-.12	-.69	25000	0109	808
#46 AM350-496 BHN	390	.098	-.102	-.42	26000	0164	183
#47 18% Nickel Maraging 450 BHN	240	.3	-.065	-.62	27000	0118	284
#48 2024-T351 Aluminum	160	.22	-.124	-.59	10600	.0148	157
#49 7075-T6 Aluminum	191	.19	-.126	-.52	10300	.0176	184
#50 SAE1005-HRLC	93	.1	-.104	-.39	29000	1.69×10	103608
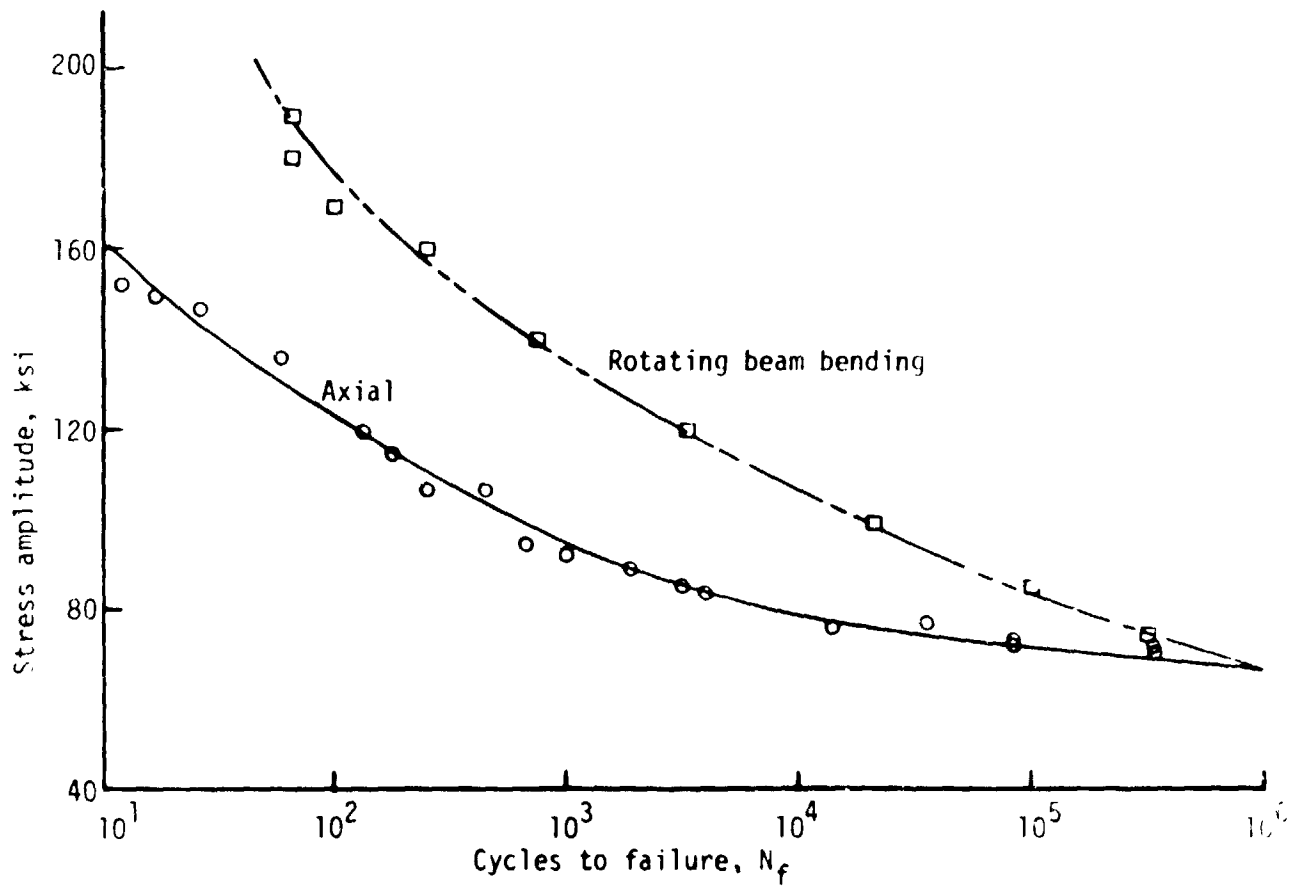
Fig. 1. Fatigue data under axial loading and in rotating bending
for 4130 steel from Ref. 1.

$$\frac{\Delta\varepsilon}{2} = \frac{\sigma_f}{E}(2N_f)^b + \varepsilon_f{}'(2N_f)^c$$
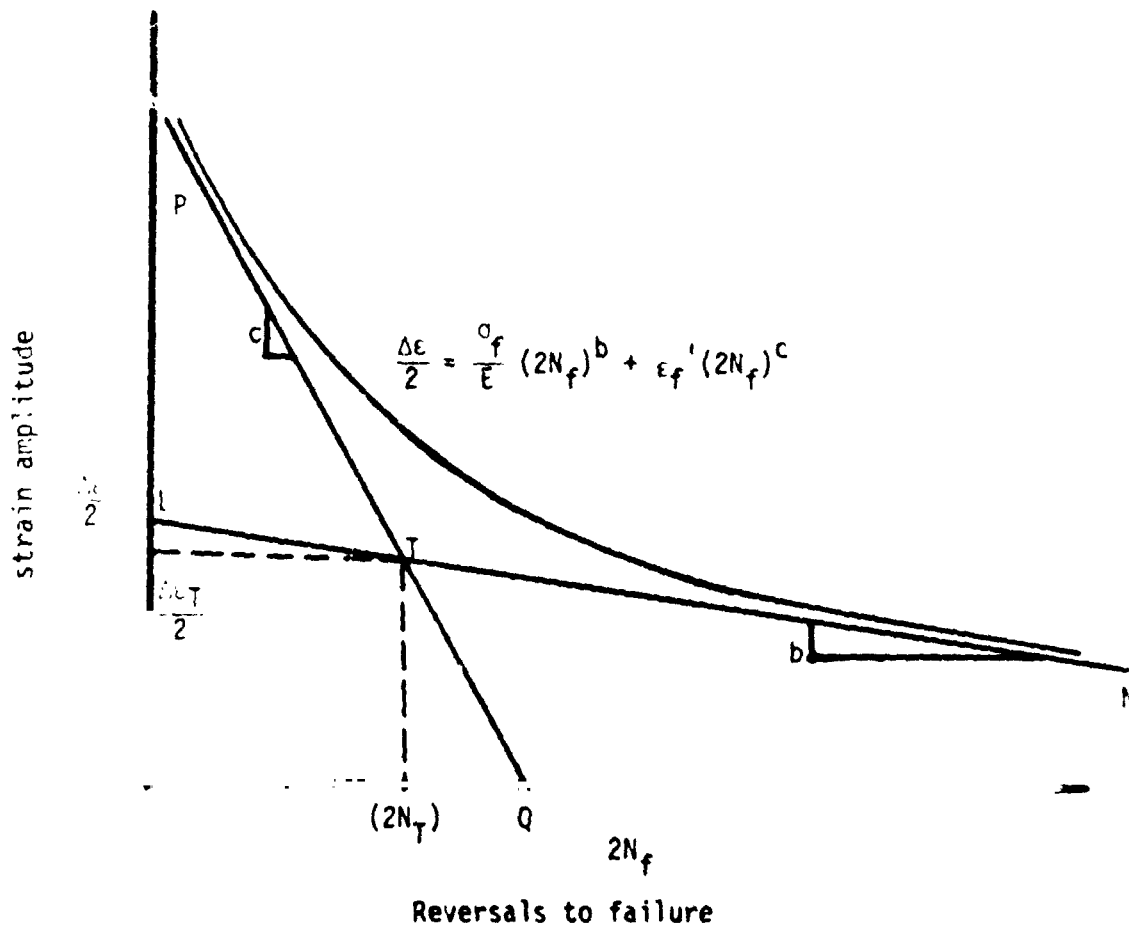
Fig. 2. Model of fatigue life relationship consisting of linear elastic and plastic components on double logarithmic coordinates.
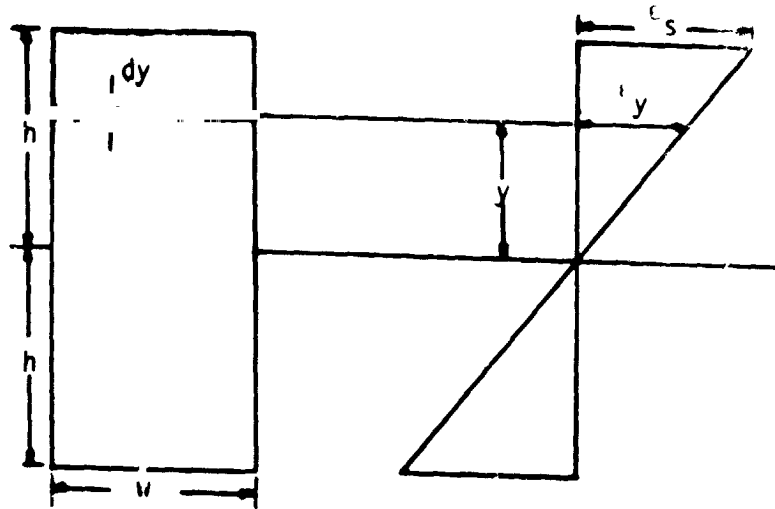
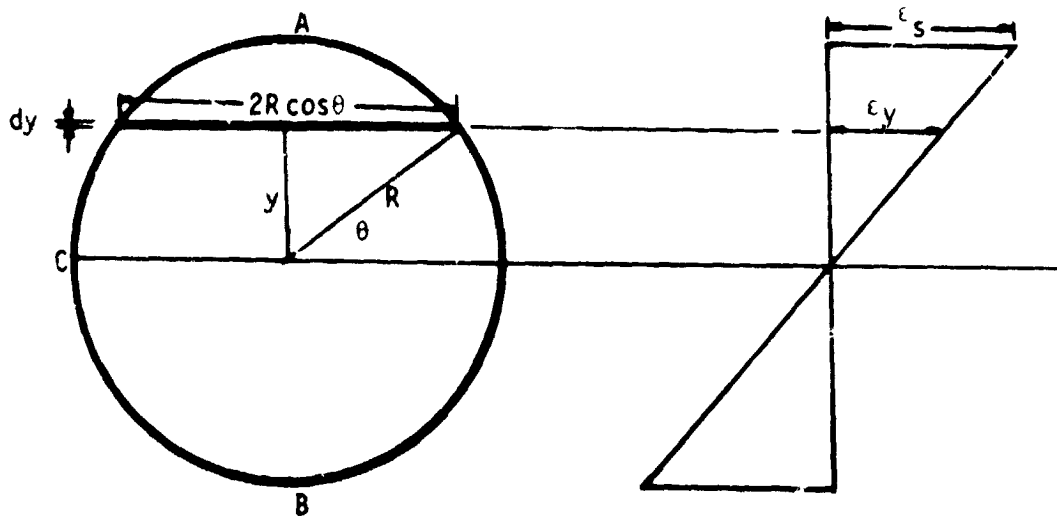Fig. 3. Rectangular cross-sectional bar in flexural bending.

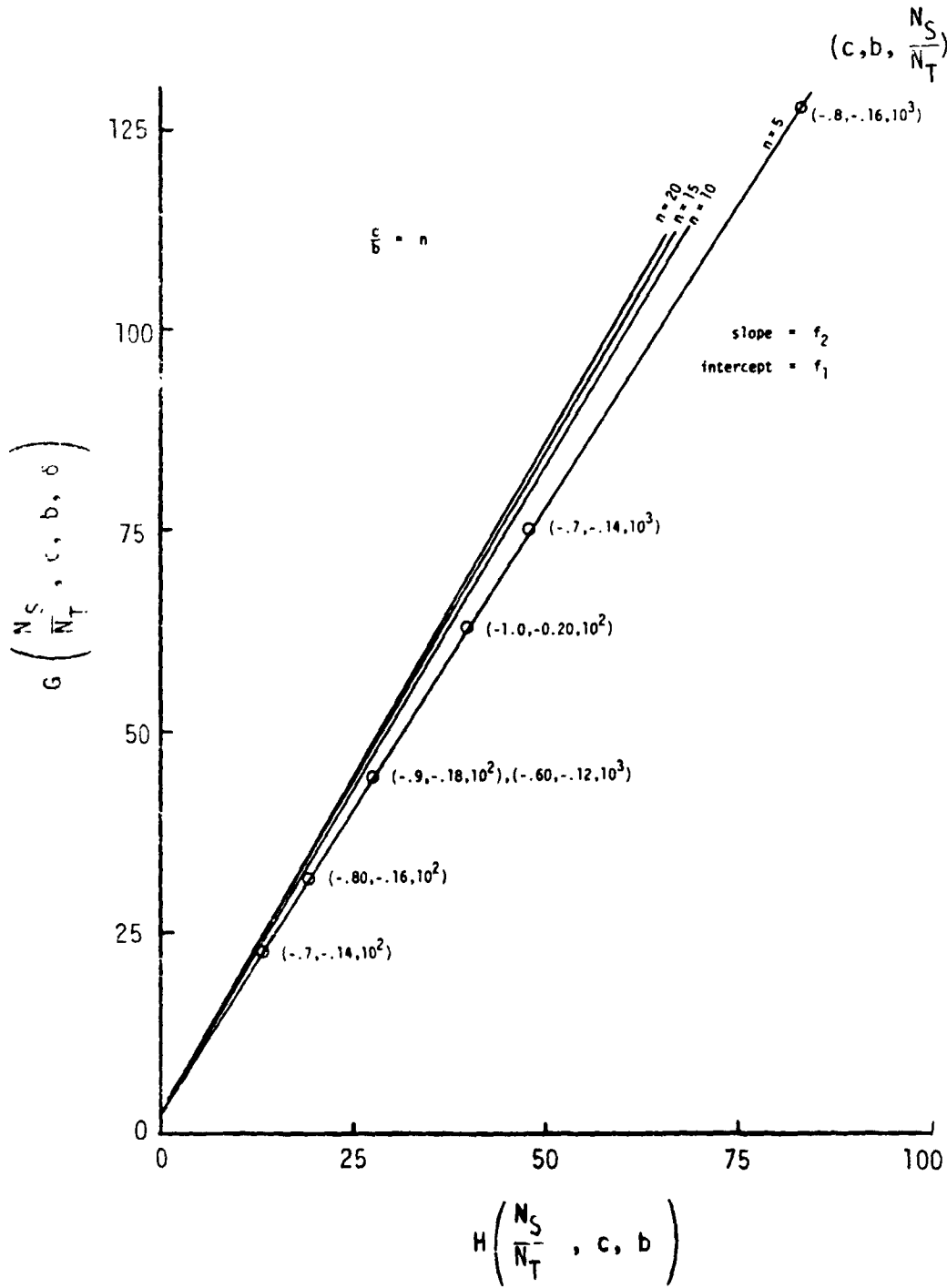
Fig. 4. Circular cross-sectional bar in flexural bending.

Fig. 5. Plot of G vs. H for a given c/b and for all combinations of c, b and (N_S/N_T) showing f_1 and f_2 are functions of only (c/b).
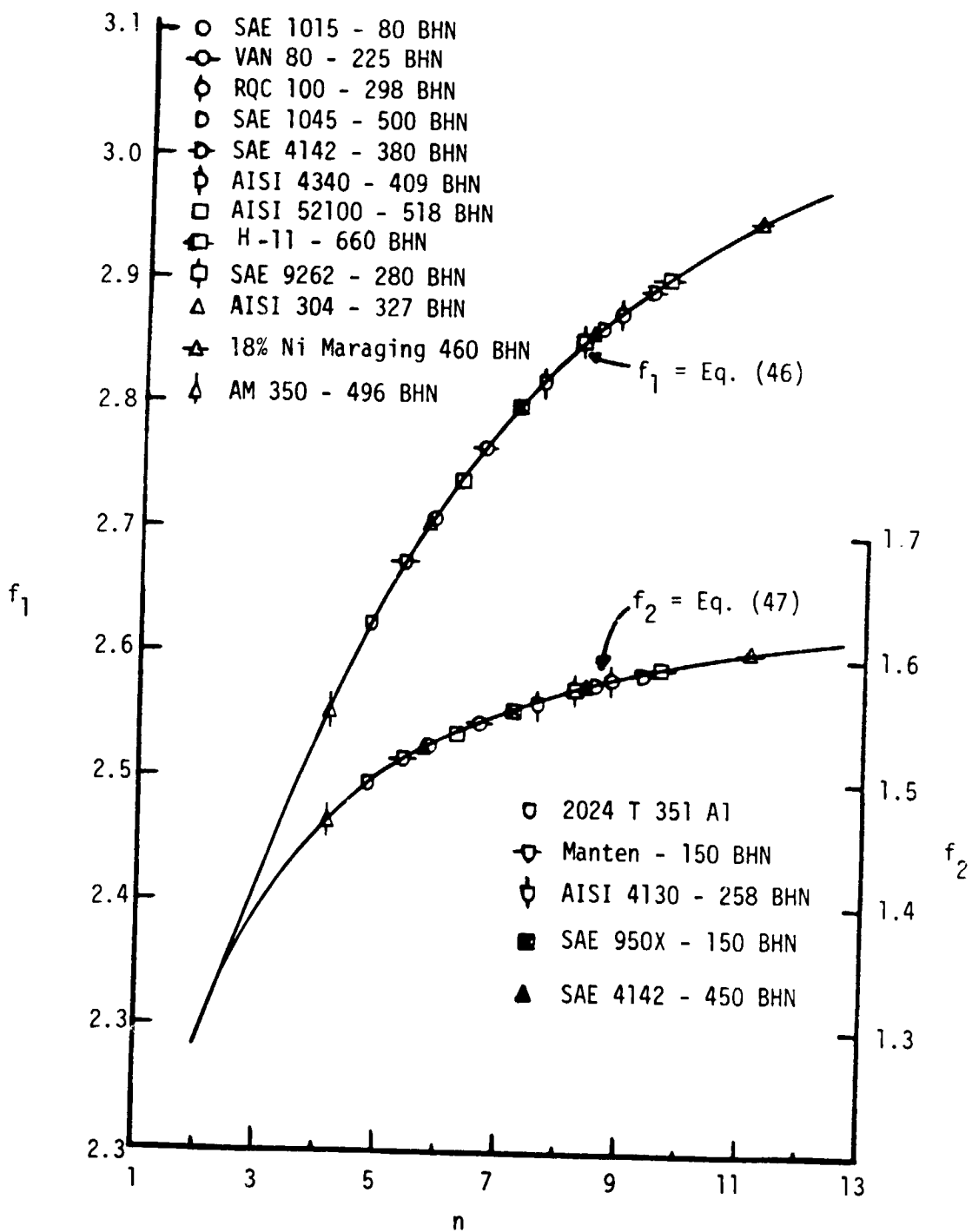
Fig. 6. The parameters f_1 and f_2 are shown for materials with different n values. The solid lines are curve-fits given by Eqs. (46) and (47), respectively.
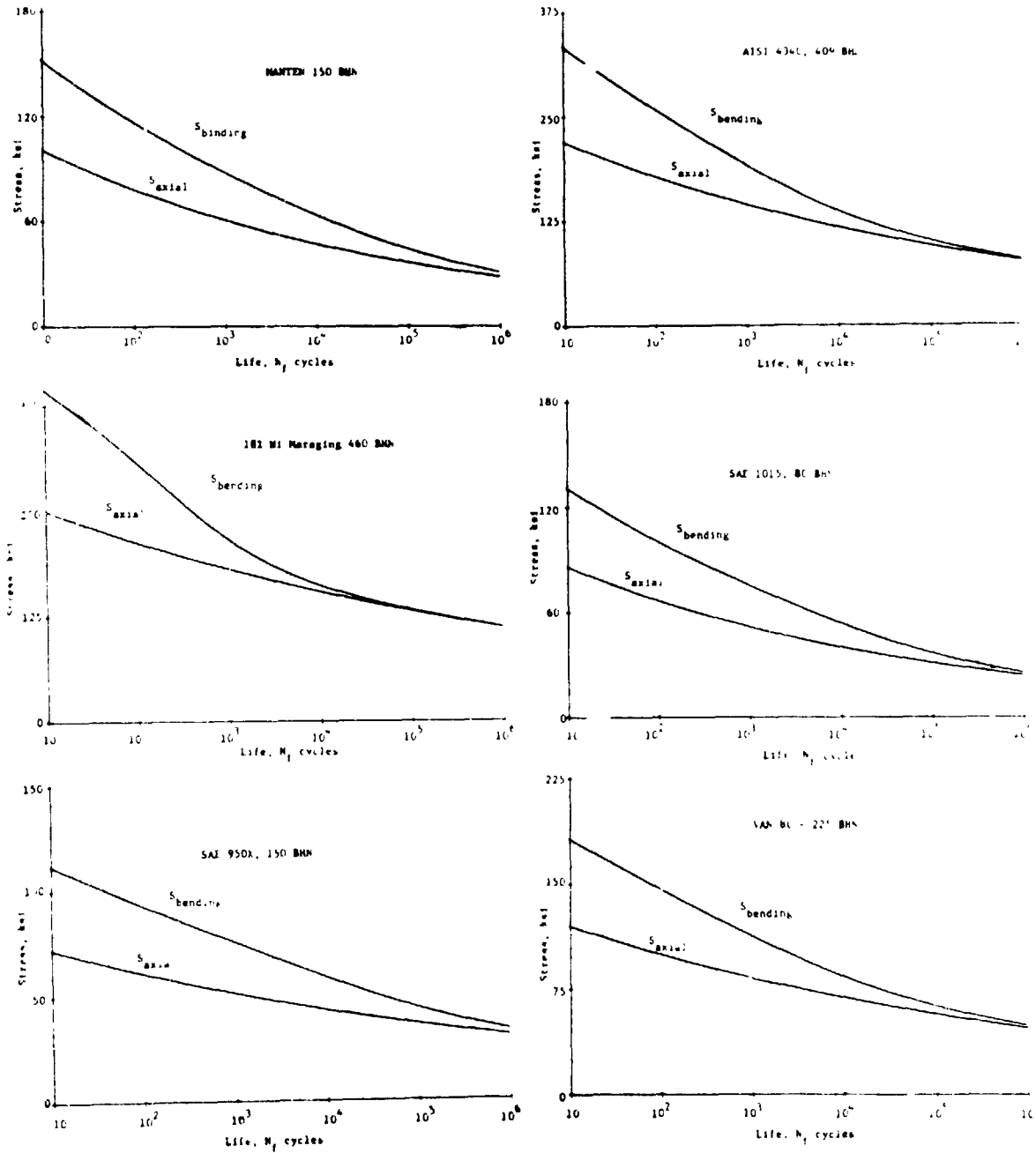
Fig. 7. Axial stress and nominal bending stress are plotted against life for various materials using formulas summarized in Table I.

Fig. 7 (Continued)

Fig. 7 (Continued)

Fig. 7 (Continued)

Fig. 7 (Continued)

Fig. 7 (Continued)

Fig. 7 (Continued)

Fig. 7 (Continued)